◆ Human Brain Mapping 38:1574–1587 (2017) ◆

Spectroscopic Biomarkers of Motor Cortex Developmental Plasticity in Hemiparetic Children after Perinatal Stroke

Helen L. Carlson,[1,2,3,4]* Frank P. MacMaster,[2,4,5,6,7,8,9] Ashley D. Harris,[2,5,8,10] and Adam Kirton[1,2,3,4,5]

[1]*Calgary Pediatric Stroke Program, Alberta Children's Hospital, Calgary, AB, Canada*
[2]*Alberta Children's Hospital Research Institute (ACHRI), AB, Canada Calgary*
[3]*Neurosciences, Alberta Children's Hospital, Calgary, AB, Canada*
[4]*Department of Pediatrics, University of Calgary, Calgary, AB, Canada*
[5]*Hotchkiss Brain Institute, University of Calgary, Calgary, AB, Canada*
[6]*Department of Psychiatry, University of Calgary, AB, Canada*
[7]*The Mathison Centre for Mental Health Research and Education, University of Calgary, Calgary, AB, Canada*
[8]*Child and Adolescent Imaging Research (CAIR) Programs, Alberta Children's Hospital, Calgary, AB, Canada*
[9]*Strategic Clinical Network for Addictions and Mental Health, Alberta Health Services, Calgary, AB, Canada*
[10]*Department of Radiology, University of Calgary, Calgary, AB, Canada*

Abstract: Perinatal stroke causes hemiparetic cerebral palsy and lifelong motor disability. Bilateral motor cortices are key hubs within the motor network and their neurophysiology determines clinical function. Establishing biomarkers of motor cortex function is imperative for developing and evaluating restorative interventional strategies. Proton magnetic resonance spectroscopy (MRS) quantifies metabolite concentrations indicative of underlying neuronal health and metabolism in vivo. We used functional magnetic resonance imaging (MRI)-guided MRS to investigate motor cortex metabolism in children with perinatal stroke. Children aged 6–18 years with MRI-confirmed perinatal stroke and hemiparetic cerebral palsy were recruited from a population-based cohort. Metabolite concentrations were assessed using a PRESS sequence (3T, TE = 30 ms, voxel = 4 cc). Voxel location was guided by functional MRI activations during finger tapping tasks. Spectra were analysed using LCModel. Metabolites were quantified, cerebral spinal fluid corrected and compared between groups (ANCOVA) controlling for age. Associations with clinical motor performance (Assisting Hand, Melbourne, Box-and-Blocks) were assessed. Fifty-two participants were studied (19 arterial, 14 venous, 19 control). Stroke participants demonstrated differences between lesioned and nonlesioned motor cortex *N*-acetyl-aspartate [NAA mean concentration = 10.8 ± 1.9 vs. 12.0 ± 1.2, $P < 0.01$], creatine [Cre 8.0 ± 0.9 vs. 7.4 ± 0.9, $P < 0.05$] and *myo*-Inositol [Ins 6.5 ± 0.84 vs. 5.8 ± 1.1, $P < 0.01$]. Lesioned motor cortex NAA and creatine were strongly correlated with motor performance in children with arterial but not venous strokes. Interrogation of motor cortex by fMRI-guided MRS is feasible in children with perinatal stroke.

Contract grant sponsors: Heart and Stroke Foundation of Canada and the Alberta Children's Hospital Foundation.

*Correspondence to: Dr. Helen L. Carlson, Department of Neurosciences, Alberta Children's Hospital, 2888 Shaganappi Trail NW, Calgary, AB, Canada T3B 6A8. E-mail: helen.carlson@albertahealthservices.ca

Received for publication 9 March 2016; Revised 20 October 2016; Accepted 7 November 2016.

DOI: 10.1002/hbm.23472

Published online 17 November 2016 in Wiley Online Library (wileyonlinelibrary.com).

Metabolite differences between hemispheres, stroke types and correlations with motor performance support functional relevance. MRS may be valuable in understanding the neurophysiology of developmental neuroplasticity in cerebral palsy. *Hum Brain Mapp 38:1574–1587, 2017*.

Key words: pediatric; magnetic resonance imaging; neuroimaging; magnetic resonance spectroscopy; spectroscopy; hemiparesis; cerebral palsy

INTRODUCTION

Perinatal strokes are focal, vascular brain injuries occurring between 20 weeks gestation and 28 days of life [Raju et al., 2007]. Most survivors incur lifelong motor disabilities and perinatal stroke accounts for the majority of hemiparetic cerebral palsy [Kirton and DeVeber, 2013]. Perinatal stroke is common (up to 1:1,600 live births) [Lynch, 2009] but pathophysiology is poorly understood and there are no prevention strategies, resulting in a large, ongoing burden. Modern neuroimaging has defined specific perinatal stroke diseases [Kirton et al., 2008]. Periventricular venous infarctions (PVI) are small subcortical strokes affecting periventricular white matter and occur in utero prior to 32–34 weeks [Kirton et al., 2008]. In contrast, arterial ischemic strokes of the middle cerebral artery typically occur near term and damage large cortical and subcortical structures [Kirton et al., 2011]. Such arterial strokes can present acutely at birth (neonatal arterial ischemic stroke, NAIS) or later in infancy (arterial presumed perinatal ischemic stroke, APPIS) but lesions are similar. Both arterial strokes and PVI typically injure one or more components of the motor system, resulting in contralateral hemiparesis (cerebral palsy).

An otherwise healthy brain sustaining a focal, unilateral injury of defined timing affords a unique opportunity to explore developmental neuroplastic mechanisms. Perinatal stroke represents such an ideal model and converging evidence from preclinical and human studies are advancing functional models of how the motor system develops following such injuries [Eyre, 2007; Kirton, 2013; Staudt, 2007]. Motor system development often includes persistence of the ipsilateral upper motor neuron connections from the nonlesioned hemisphere to the affected limbs that are present at birth but otherwise withdrawn during early development. As a result, the integrity and relative contribution of both the lesioned and nonlesioned motor cortices are often regarded as essential, functionally relevant "hubs" within the developing motor network following perinatal stroke.

Improving our understanding of these mechanisms of endogenous developmental neuroplasticity is essential if outcomes are to be improved. Treatment options for childhood hemiparesis are limited but the translational significance of these models is increasingly evident. Multiple rehabilitation trials based on these models have recently shown promise in improving motor function. Two randomized, controlled trials of noninvasive motor cortex stimulation have demonstrated additive effects on motor learning in children with perinatal stroke and hemiparesis [Gillick et al., 2014; Kirton et al., 2016b]. Comprehensive imaging models of developmental plastic reorganization also appear predictive of how young hemiparetic patients respond to evidence-based interventions such as constraint-induced movement therapy [Juenger et al., 2013]. Establishing valid, reliable biomarkers of baseline functioning and mechanisms of change is imperative for assessing effectiveness and guiding future development of rehabilitation strategies.

While brain mapping with transcranial magnetic stimulation and other neurophysiology tools have been essential, the above progress has been predominantly facilitated by advances in neuroimaging. Functional MRI (fMRI) uses task-related changes in the blood oxygen-level dependent (BOLD) response to map locations of functional areas (such as motor cortex) that may be displaced from traditional anatomical locations through reorganization after injury. Resting state fMRI may use the BOLD signal to explore functional connectivity following stroke [Biswal et al., 1995; Westlake and Nagarajan, 2011] while diffusion tensor imaging (DTI) adds structural connectivity information [Kumar et al., 2016]. Converging evidence from these MR modalities can inform on neuroplastic mechanisms occurring following stroke. However, they have mainly been applied to the adult brain and none are able to interrogate regional brain metabolism.

Additional neuroimaging technologies have further increased our understanding of neural networks and their reorganization following stroke in adults. One such method, proton (^{1}H) magnetic resonance spectroscopy (MRS), quantifies *in vivo* metabolite concentrations within a brain region of interest. Measuring metabolite concentrations with MRS can provide information on neuronal health (*N*-acetyl-aspartate [NAA]), cell membrane turnover (choline compounds [GPC + PCh]), energy metabolism (creatine compounds [Cr + PCr]), metabolic activity and excitatory neurotransmitter concentration (glutamate/glutamine [Glx]) and health of glial cells (*myo*-Inositol [Ins]) among others [Dani and Warach, 2014; Rae, 2014]. MRS metabolism markers have been associated with neurological outcomes in adult stroke such as NAA and Ins correlations with motor outcomes [Cirstea et al., 2011; Craciunas et al., 2013; Kang et al., 2000; Kobayashi et al., 2001]. Early evidence suggests similar potential utility in childhood central nervous system injury [Holshouser et al., 1997]. However, MRS applications following early brain injury have been limited [Shu et al., 1997] and systematic applications to the specific injuries of perinatal stroke have not been described.

The aim of this study was to examine the metabolite properties of bilateral motor cortex after perinatal stroke and their relationship to clinical function. We hypothesized that as a biomarker of neuronal integrity, NAA would be higher in typically developing controls compared to lesioned motor cortex of children with perinatal stroke and positively associated with motor outcomes.

METHODS

Participants

Participants with perinatal stroke were recruited via the Alberta Perinatal Stroke Project (APSP), a population-based research cohort. Inclusion criteria were: (1) unilateral, MRI-confirmed perinatal stroke syndrome according to previously validated criteria [Kirton et al., 2008] including NAIS, APPIS, or PVI, (2) age 6 to 19 years, (3) symptomatic hemiparesis Pediatric Stroke Outcome Measure (PSOM) score >0.5 [Kitchen et al., 2003] AND Manual Ability Classification System (MACS) score I–IV [Arner et al., 2005] AND perceived functional limitations by both child and parent] and (4) informed consent/assent. Children with additional neurodevelopmental or psychiatric conditions, unstable epilepsy or hemiparesis intervention (e.g., orthopedic surgery, botulinum toxin) within 12 months were excluded.

Typically developing (TD) volunteers were recruited through an established healthy controls program. TD participants were right handed, aged 6 to 19 years and had no neurodevelopmental or psychiatric conditions or MRI contraindications. TD participants were gender and age matched (±1 year) with PS participants.

Written parental consent (and subject assent when applicable) was obtained. This study was approved by the Conjoint Health Research Ethics Board, University of Calgary.

Imaging

Images were acquired at the Alberta Children's Hospital Diagnostic Imaging Suite using a 3.0 Tesla GE Discovery MR750w MRI scanner (GE Healthcare, Waukesha, WI) with an MR Instruments (Minnetonka, MN) 32-channel receive-only head coil. High-resolution anatomical T1-weighted fast spoiled gradient echo (FSPGR) images were acquired in the axial plane [166 slices, no skip; voxel size = 1.0 mm isotropic; repetition time (TR) = 8.5 ms; echo time (TE) = 3.2 ms; flip angle = 11°; field of view (FOV) = 256 mm^2; matrix = 256 × 256].

Task functional MRI

Task fMRI acquisition used 137 T2*-weighted whole brain echo planar volumes (EPI; 36 interleaved contiguous slices; voxel size = 3.6 mm isotropic; TR = 2,000 ms; TE = 30 ms; flip angle = 60°; matrix = 64 × 64). Five volumes (10 s) were discarded at the beginning of each functional run to attain magnetic field equilibrium.

Participants viewed a grey screen with a fixation cross at the centre. During task blocks (12 s in duration), the cross changed from red to green (frequency ~1 Hz) and participants were asked to tap a button with their index finger in synchrony with the changing colour of the cross. In the case of profound motor impairment in which pressing with the index finger was difficult, participants were allowed to engage their wrist and/or forearm to achieve the press. Rest blocks were passive viewing of a red fixation cross for 24 s. Eight blocks of rest and seven blocks of task were interleaved, lasting approximately 5 min. Two uni-manual tapping sessions were completed, one for each hand.

Task-based functional analyses were performed on the scanner console using Brainwave (GE Healthcare) allowing real-time processing, monitoring of head motion and display of BOLD activation patterns during the tapping tasks. The MRS voxels were subsequently positioned on the highest areas of activation identified during the tapping task in the same scanning session.

MR spectroscopy

MRS data were acquired in two 20 × 20 × 10 mm^3 voxels using a standard point-resolved single voxel spectroscopy (PRESS) sequence (TR/TE = 2,000/30 ms, 128 averages) and eight unsuppressed water scans for quantification. MRS voxels were placed using the T1 anatomical image overlaid with task-related BOLD activations from the right and left hand tapping tasks (described above). The location of highest BOLD activation during the left hand tapping task was used to position the MRS voxel in the right hemisphere (typically the "hand knob" of the pre-central gyrus) [Yousry et al., 1997]. The same procedure was used to position the MRS voxel in the left hemisphere but utilizing the BOLD activation during a right hand tapping task. For participants that had no activations in pre-central gyrus (or had no cortex) for a given side, the closest BOLD activation (typically in perilesional cortex) was used to position the voxel. Figure 1 illustrates typical MRS voxel placement.

MRS spectra were generated and analyzed using LCModel [Provencher, 2001]. Metabolites were quantified using two references; first using a water reference (reported in institutional units [i.u.]), and second using a creatine reference (reported in ratios to Cre). Metabolites measured were: *N*-acetyl-aspartate [NAA], creatine-containing compounds [creatine + phosphocreatine: Cr + PCr], choline compounds [glycerophosphocholine + phosphocholine: GPC + PCh], *myo*-Inositol [Ins] and glutamate/glutamine [Glx]. Only those metabolites with estimated standard deviations (Cramér-Rao lower bounds) that did not exceed 15% for any patient were analyzed.

After coregistering and segmenting the T1-weighted image (using SPM8; Wellcome Trust Centre for Neuroimaging, UCL, UK), the voxel cerebral spinal fluid (CSF), white

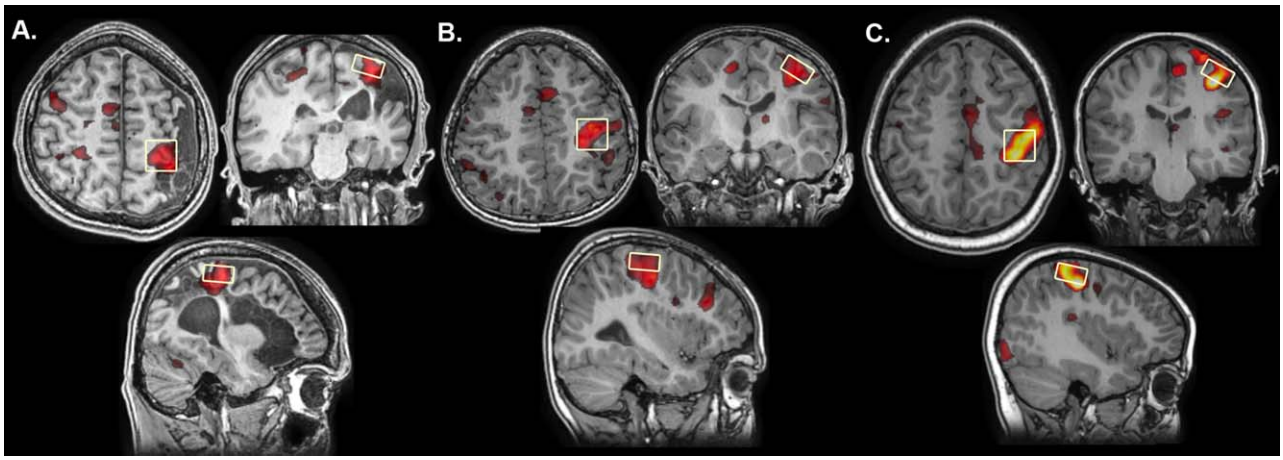

Figure 1.

Function-guided MRS voxel placement. MRS voxel placement viewed on axial, coronal and sagittal slices approximates the hand-knob in the precentral gyrus in a representative (**A**) Arterial, (**B**) PVI and (**C**) TD participant. Voxels were placed corresponding to task fMRI activations measured during a finger tapping task. Lesioned hemispheres have all been reoriented to the right side.

(WM) and grey matter (GM) fractions were determined by overlaying a binary MRS voxel mask onto the T1-weighted image using a customized version of Gannet 2.0 [Harris et al., 2015]. Metabolite concentrations were then CSF-corrected as follows: corrected metabolite concentration = metabolite concentration/(1-$CSF_{fraction}$) [Cirstea et al., 2011].

To quantify the degree of overlap of MRS voxels across participant group and hemisphere, individual T1-weighted images were coregistered to a standard paediatric template atlas in Montreal Neurological Institute (MNI) space [Fonov et al., 2011] using SPM8 and the same transformation matrix was applied to the MRS voxel masks. In-house MATLAB scripts (version R2014a, The Mathworks) then calculated the Dice similarity coefficient. This index is analogous to the Jaccard coefficient and represents the amount of overlap (i.e., MRS voxel A and B) divided by the union (i.e., MRS voxel A or B) of two voxels. Dice coefficients were calculated as follows: $DC = (A \cap B)/(A \cup B)$ where A is the voxel mask for the exemplar voxel (from a representative TD control subject) and B is the voxel mask for comparison. Larger Dice similarity coefficients indicate a greater extent of voxel overlap in three dimensions.

Motor Function

Motor function was assessed for all stroke participants by experienced, certified pediatric occupational therapists. Three evidence-based, validated motor function tasks were used; the Assisting Hand Assessment (AHA), the Melbourne Assessment of Unilateral Upper Limb Function (MA) and the Box and Blocks Test of Manual Dexterity (BBT). All sessions were videotaped and scored offline by observers blinded to stroke type and imaging outcomes. For all motor functioning tasks, higher scores indicate better performance.

The AHA is a 22-item assessment tool that measures spontaneous bimanual hand function in children with motor impairments [Holmefur et al., 2007; Krumlinde-sundholm and Eliasson, 2003; Krumlinde-sundholm et al., 2007]. It has the advantage of using real-world activities to measure spontaneous bimanual motor function rather than testing the affected hand in isolation. Motor outcomes were quantified and converted to AHA logit units (log-odds probability units) ranging from 0 (hand is not used at all) to 100 (normal motor function).

The MA consists of 16 tasks that measure motor function in unilateral hemiparetic upper limbs [Bourke-Taylor, 2003; Randall et al., 1999]. Typical tasks include reaching and grasping different sized objects reflecting finger dexterity and speed of motion. Raw scores range from 0 (no achievement of tasks) to 122 points (no impairment) and were expressed as percentages [MA = (# of points achieved/total # points possible)*100].

The BBT is a performance-based measure of upper limb dexterity in which participants move a series of blocks from one container into another as quickly as possible [Mathiowetz et al., 1985]. A final score was generated for both the affected (BBT-A) and unaffected (BBT-U) hands by counting the number of blocks successfully transferred in 60 s.

Statistical Analyses

Distribution normality tests were performed (Shapiro–Wilk). Pearson bivariate correlations explored the relationships between age and metabolite concentrations. Mixed design analyses of covariance (ANCOVAs) were used to investigate the main effects of metabolite concentrations (NAA, Cre, Ins, Cho, Glx), patient group (arterial, PVI, TD) and hemisphere

TABLE I. Demographic characteristics and motor function of participant groups

	Participant group		
Category	Arterial	PVI	TD
Mean age (SD) [range]	13.53 (4.2) [6.8–19.0] years	12.47 (4.1) [6.6–19.7] years	12.72 (3.7) [6.0–19.0] years
Sex [%]			
Male	$N = 11$ [57.9%]	$N = 10$ [71.4%]	$N = 10$ [53.0%]
Female	$N = 8$ [42.1%]	$N = 4$ [28.6%]	$N = 9$ [47.0%]
Total	$N = 19$	$N = 14$	$N = 19$
Side of stroke (MRI) [%]			
Right	$N = 8$ [42.1%]	$N = 8$ [57.1%]	–
Left	$N = 11$ [57.9%]	$N = 6$ [42.9%]	–
AHA Mean (SD) [range]	60.06 (19.0) [35–100]	72.31 (16.3) [55–100]	–
MA Mean (SD) [range]	71.60 (21.2) [40.5–100]	87.21 (10.6) [66.3–100]	–
BBT Mean (SD) [range]			
Affected	19.67 (16.0) [1–52]	31.38 (9.9) [17–49]	–
Unaffected	47.61 (10.9) [31–69]	52.70 (16.9) [19–84]	–

Notes: SD, Standard deviation; PVI, Periventricular venous infarction; TD, Typically developing; MRI, MRI confirmed diagnosis of stroke and side; AHA, Assisting Hand Assessment; MA, Melbourne Assessment of Unilateral Upper Limb Function; BBT, Box and Block Test of Manual Dexterity.

(lesioned/nondominant vs. nonlesioned/dominant) as well as their interactions (controlling for age). Pearson's partial correlation coefficients assessed the relationship between metabolite concentrations and motor outcomes (MA, AHA, BBT-A, BBT-U) controlling for age. Independent samples *t*-tests compared Dice similarity coefficients (i.e., degree of voxel overlap) between groups. The Statistical Package for the Social Sciences (IBM SPSS Version 19 for Windows, Chicago) was used to perform all analyses.

RESULTS

Population

Both MRS voxels from one participant were excluded due to poor MRS data quality resulting from excessive head motion and lipid contamination. The final population consisted of 52 participants; 19 with arterial strokes [mean age (SD) = 13.53 (4.2) years], 14 with venous strokes [mean age (SD) = 12.47 (4.1) years] and 19 TD controls [mean age (SD) = 12.72 (3.7) years]. Table I contains additional demographic variables.

Metabolite Levels

Cramér–Rao bounds ranged between 4% and 13% for all metabolites indicating good fit for estimated models. Figure 2 illustrates three sample spectra for the lesioned/nondominant hemisphere for each patient group. Task fMRI-driven voxel placement was highly consistent across participants. Figure 3 illustrates the centre of mass for each voxel by patient group. Dice similarity coefficients (DC) of MRS voxel overlap in the lesioned/nondominant hemisphere were significantly higher (indicating more overlap) for TD controls [mean DC (SD) = 0.23(0.1), $t(35) = 4.2$, $P < 0.01$] and PVI patients [mean DC (SD) = 0.33(0.1), $t(35) = 3.5$, $P < 0.01$] compared to arterial participants [mean DC (SD) = 0.17(0.1)]. No group differences in DC were found for the nonlesioned/dominant hemisphere.

The proportion of CSF in MRS voxels was similar for all patient groups between hemispheres [mean CSF(SD) = 0.17 (0.07)] although TD controls had significantly less CSF for the nondominant hemisphere ($Z = 2.2$, $P < 0.05$) compared to dominant. Proportions of GM and WM across patient groups and hemispheres are shown in Table II.

Pearson correlation coefficients between age and metabolite concentrations revealed a significant relationship for Glx in the nondominant hemisphere of control participants ($r = -0.64$, $P < 0.01$). As other metabolites showed statistical trends toward significance (e.g., Cre: $r = 0.42$, $P = 0.07$), age was included as a covariate in subsequent analyses.

A mixed model ANCOVA of metabolite concentrations (water referenced) revealed a significant three-way interaction between hemisphere, metabolite and patient group [$F(8,92) = 4.35$, $P < 0.01$] controlling for age. Subsequent *post hoc* analyses were performed to examine more specific differences in metabolite concentrations between hemispheres in each patient group (Fig. 4). Metabolite levels using Cre as a reference are presented in Figure 5 for comparison and are summarized below.

Water-Referenced Metabolite Levels

NAA results are summarized in Figure 4A for concentrations using the water signal as a reference. In TD participants, NAA was asymmetrical, being lower in the nondominant hemisphere compared to the dominant hemisphere ($P < 0.01$). Participants with arterial stroke showed lower concentrations of NAA in the lesioned hemisphere ($P < 0.01$) compared to the intact hemisphere.

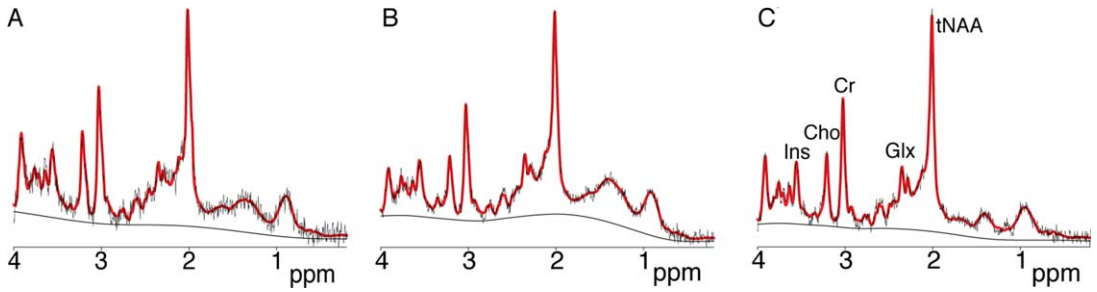

Figure 2.

Sample spectra from the lesioned/nondominant hemisphere of (**A**) arterial, (**B**) PVI and (**C**) TD participants. LCM fit in red overlaid on raw data in black as well as baseline. [Color figure can be viewed at wileyonlinelibrary.com]

Participants with PVI showed no NAA concentration differences between hemispheres. In the PVI group, NAA in the lesioned side was significantly higher than the arterial group ($P < 0.05$), and more similar to the TD group. In the nonlesioned hemisphere of the PVI group, NAA values were lower than the dominant hemisphere of controls ($P < 0.05$) with a similar statistical trend observed in the arterial group ($P = 0.06$).

Cre concentrations (Fig. 4B) were also asymmetrical in TD controls, again being lower in the nondominant hemisphere ($P < 0.05$). In contrast, concentrations of Cre in the PVI group were higher in the lesioned hemisphere ($P < 0.05$).

Ins concentrations between hemispheres were comparable in both PVI and TD controls. In the arterial group, Ins concentrations were higher in the lesioned hemisphere compared to nonlesioned ($P < 0.01$, Fig. 4C).

Choline compounds also showed asymmetry in TD participants; levels were higher in the dominant hemisphere compared to nondominant ($P < 0.01$, Fig. 4D). Levels in the lesioned hemisphere for both arterial ($P < 0.01$) and PVI ($P = 0.06$) were higher than for the nondominant hemisphere in TD, although for PVI this did not reach statistical significance. Glx concentrations were comparable between hemispheres and groups (Fig. 4E).

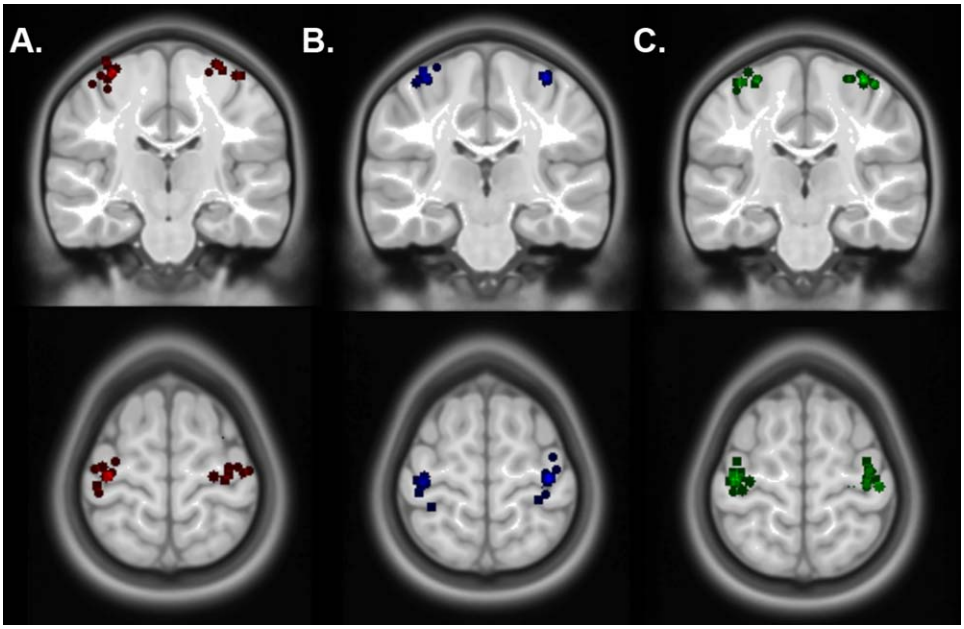

Figure 3.

MRS voxel placement by patient group. Dispersion maps illustrating voxel placement by patient group (overlaid on a standard template image). Each marker represents the centre of mass of each voxel for (**A**) arterial, (**B**) PVI and (**C**) TD participants on coronal and axial slices. Lesioned hemisphere markers have been reoriented to the right side. Note that some markers are not visible on the currently selected slice. [Color figure can be viewed at wileyonlinelibrary.com]

TABLE II. Tissue fractions within MRS voxels and relation to motor function

Tissue fractions	Mean CSF (SD)	Mean GM (SD)	Mean WM (SD)
TD Controls			
Nondominant	0.17 (0.08)	0.38 (0.07)	0.45 (0.08)
Dominant	0.20 (0.07)	0.41 (0.07)	0.39 (0.06)
Hemispheric difference	$Z = 2.2$, $P < 0.05$	$T(21) = 2.3$, $P < 0.05$	$T(21) = 3.6$, $P < 0.01$
Arterial			
Lesioned	0.16 (0.07)	0.44 (0.11)	0.40 (0.15)
Nonlesioned	0.15 (0.07)	0.46 (0.08)	0.39 (0.11)
Hemispheric difference	n.s.	n.s.	n.s.
PVI			
Lesioned	0.17 (0.08)	0.48 (0.05)	0.35 (0.09)
Nonlesioned	0.15 (0.06)	0.47 (0.05)	0.38 (0.09)
Hemispheric difference	n.s.	n.s.	$T(13) = 2.4$, $P < 0.05$
Correlations (lesioned)	**CSF**	**GM**	**WM**
Motor Function			
MA	$r = 0.29$, n.s.	$r = 0.74$, $P < 0.01$	$r = -0.51$, $P < 0.01$
AHA	$r = 0.17$, n.s.	$r = 0.45$, $P < 0.05$	$r = -0.43$, $P < 0.05$
BBT-A	$r = 0.26$, n.s.	$r = 0.54$, $P < 0.01$	$r = -0.54$, $P < 0.01$
Correlations (nonlesioned)	**CSF**	**GM**	**WM**
Motor Function			
MA	$r = 0.07$, n.s.	$r = 0.50$, $P < 0.01$	$r = -0.39$, $P < 0.05$
AHA	$r = 0.09$, n.s.	$r = 0.46$, $P < 0.05$	$r = -0.38$, $P < 0.05$
BBT-A	$r = 0.21$, n.s.	$r = 0.45$, $P < 0.05$	$r = -0.45$, $P < 0.05$

Notes: CSF, cerebral spinal fluid; GM, Grey matter; WM, White matter; TD, Typically developing; PVI, Periventricular venous infarction; MA, Melbourne Assessment of Unilateral Upper Limb Function; AHA, Assisting Hand Assessment; BBT-A, Box and Block Test (Affected hand); *Z*, Related-samples Wilcoxon signed rank test; *T*, paired samples *t*-test; *r*, Pearson correlation coefficient; n.s., not significant. Motor function was measured for patients with perinatal stroke only.

Cre-Referenced Metabolite Levels

Results were generally consistent between water reference and Cre reference results with a few exceptions. Hemispheric asymmetry in NAA levels for dominant versus nondominant hemispheres in controls was not present using NAA/Cre ratios. This was also true for differences in NAA levels between nondominant hemispheres in controls versus nonlesioned in PVI (Fig. 5A). As seen in the NAA water-referenced data, no group differences were found between the nonlesioned/dominant hemispheres. All other NAA differences were preserved.

For Cho/Cre, using the Cre reference revealed a significant difference between the lesioned hemispheres of arterials and PVIs ($P < 0.05$) that was not significant using a water reference. There was also a significant difference ($P < 0.01$, Fig. 5D) in controls between dominant and nondominant hemispheres for Glx when referencing using Cre.

Motor Function

Means, variances and ranges of scores for the four motor tasks in each stroke group are presented in Table I. Participants with arterial stroke had lower average performance on the MA [$t(29) = -2.4$, $P = 0.02$] and BBT-A [$t(29) = -2.34$, $P = 0.03$] compared to PVI participants. Performance on the AHA showed a similar trend [AHA: $t(29) = -1.9$, $P = 0.07$]. Unaffected hand BBT performance was comparable between stroke groups. There were positive relationships between GM fraction and motor function in both the lesioned and nonlesioned hemispheres for both arterial and PVI groups (Table II).

Metabolite and Motor Function Correlations

The relationship between lesioned motor cortex metabolites (water referenced) and clinical motor function (controlling for age) in arterial participants are shown in Figure 6 and summarized for both hemispheres (and for PVI patients) in Table III. All motor function measures for arterial patients were positively correlated with metabolite concentrations in the lesioned motor cortex with higher concentrations associated with better performance. Specifically, both NAA and Cre concentrations were positively correlated with performance on MA, AHA and BBT-A (Fig. 6A,B,C). In addition, concentrations of the lesioned motor cortex metabolites also correlated with BBT-U score reflecting the "normal hand" (Fig. 6D). Within the lesioned motor cortex, the strength of the correlation for the MA and AHA was greater for NAA as compared to Cre (Table III).

A similar pattern was seen for metabolite concentrations in the nonlesioned motor cortex. Here, the most consistent correlations were again seen for NAA where all motor outcomes were correlated. Correlations of motor function

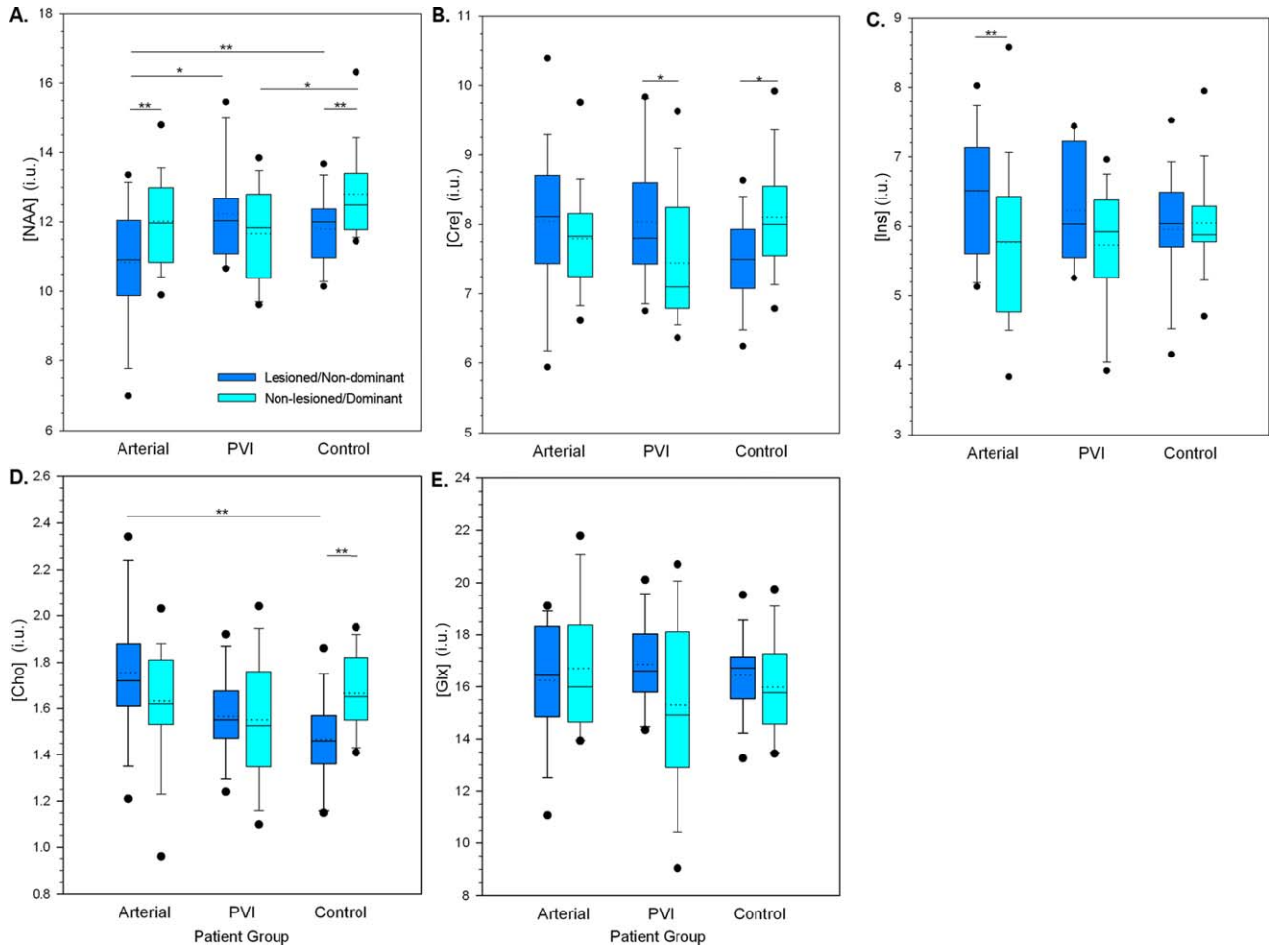

Figure 4.

Boxplots illustrating CSF-corrected metabolite concentrations (i.u.) using a water reference by patient group and hemisphere. **A**. *N*-acetyl-aspartate (NAA), **B**. Creatine compounds (Cre), **C**. *myo*-Inositol (Ins) **D**. Choline compounds (Cho), **E**. Glutamate + glutamine (Glx). Median (solid line) and mean (dotted line) concentrations as well as quartile ranges and outliers (filled circles) are displayed. ** $P < 0.01$, * $P < 0.05$. [Color figure can be viewed at wileyonlinelibrary.com]

with the nonlesioned motor cortex Cre were less evident as compared to the lesioned hemisphere.

Ins concentration in the lesioned motor cortex was associated with function in the unaffected hand as measured by BBT-U ($r = 0.64$, $P < 0.01$). No significant associations were observed between Ins or choline compound concentrations and motor function of the affected hand though several possible correlations were observed including both the AHA and BBT-A associated with Ins levels ($r = 0.47$, $P = 0.06$). Glx concentrations did not appear to be related to any motor outcome.

DISCUSSION

We have demonstrated that task fMRI-guided measurement of motor cortex metabolites is feasible in children with perinatal stroke and cerebral palsy. Participants with stroke showed significant differences between lesioned and nonlesioned hemispheres for NAA, creatine and Ins but not other metabolites. Clinical relevance is supported by consistent, metabolite-specific associations with motor performance measures in children with arterial but not venous strokes.

Of the metabolites measured, NAA appears to be the most sensitive for differentiating between patient groups, hemispheres (lesioned vs. nonlesioned) and motor function. This is consistent with past studies in adult stroke patients [Cirstea et al., 2011; Craciunas et al., 2013; Jones et al., 2016; Kang et al., 2000; Kobayashi et al., 2001]. NAA is often considered to be a marker of neuronal health, though the meaning of altered NAA levels is not fully understood. Decreased NAA is thought to reflect cell loss [Rae, 2014] and this may be consistent with our finding of

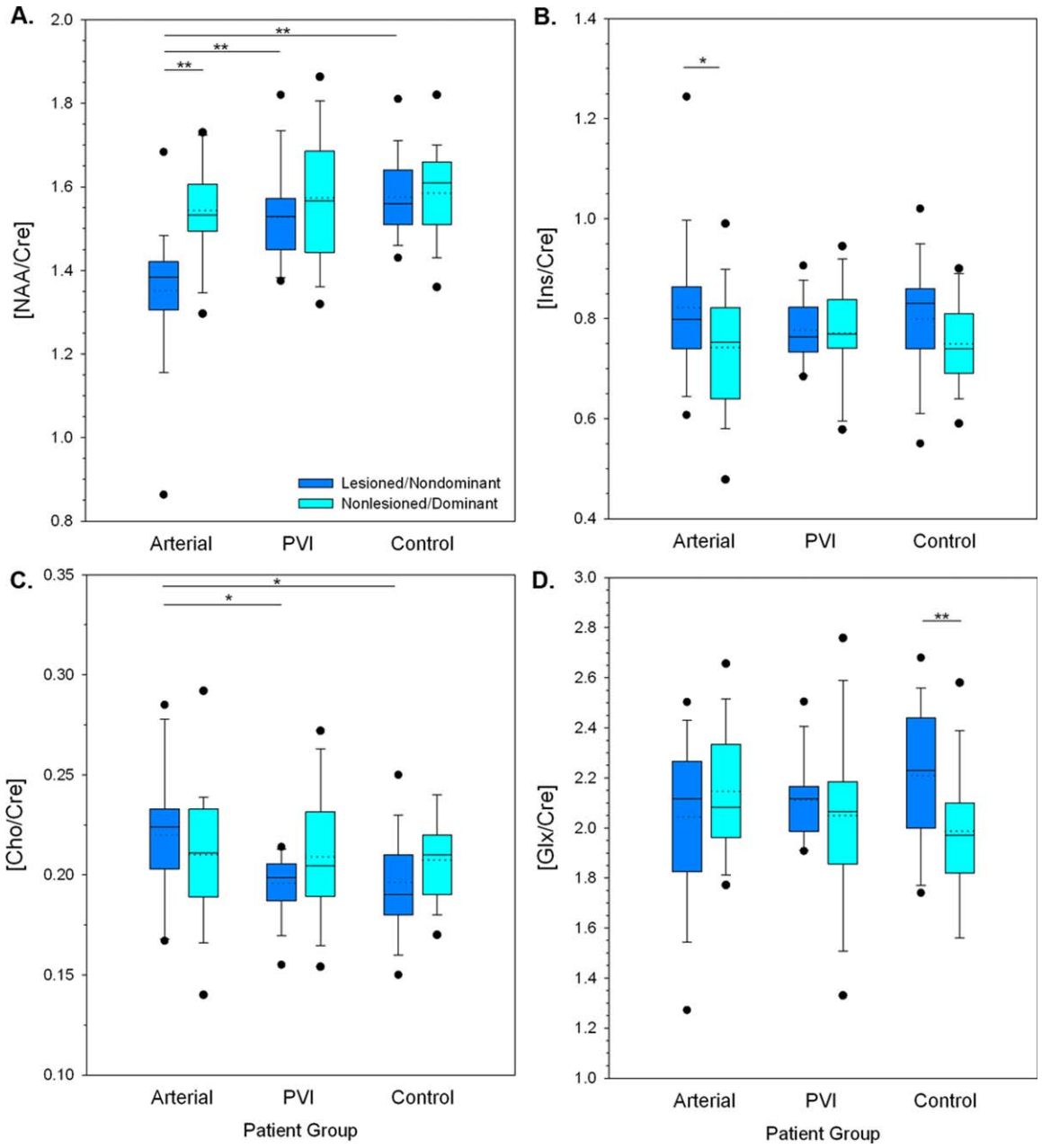

Figure 5.

A–D. Boxplots illustrating metabolite concentrations (using creatine concentration ratios) by patient group and hemisphere. A. *N*-acetyl-aspartate (NAA/Cre), B. *myo*-Inositol (Ins/Cre) C. Choline compounds (Cho/Cre), D. Glutamate + glutamine (Glx/Cre). Median (solid line) and mean (dotted line) concentrations as well as quartile ranges and outliers (filled circles) are displayed. ** $P < 0.01$, * $P < 0.05$. [Color figure can be viewed at wileyonlinelibrary.com]

decreased NAA levels in stroke hemisphere motor areas compared to contralateral tissue. However, decreased NAA is not simply a result of irrecoverable cell death/tissue infarct since NAA can increase following successful reperfusion therapy [Albers et al., 2006]. It is unknown if there is a time window for this form of tissue recovery. All patients in the current study had chronic stroke (mean time interval from birth = 13.1 (4.1) years; minimum time = 6.6 years). As such, the reduced NAA in perilesional areas and its correlation with motor function suggests

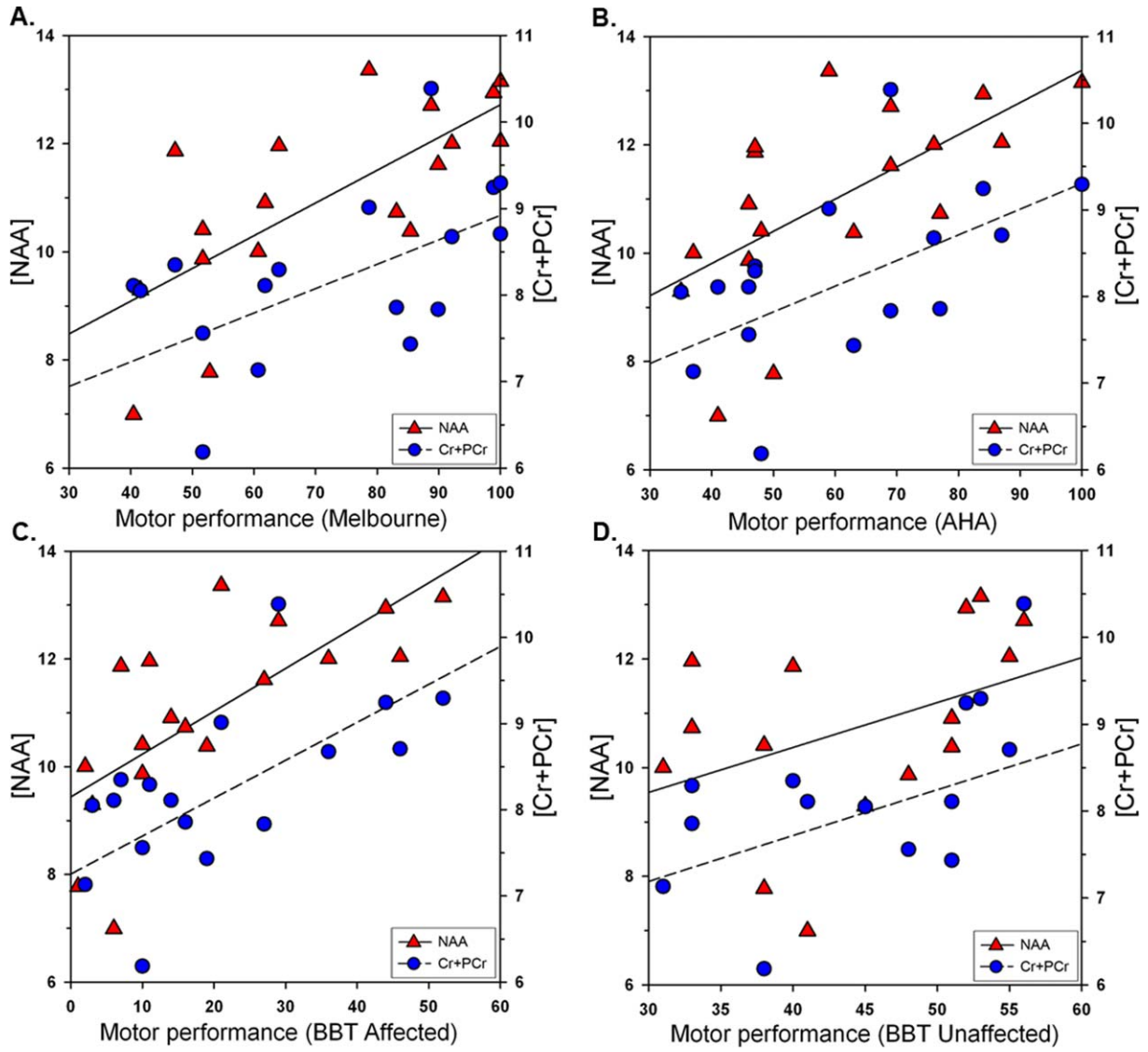

Figure 6.

Relationship between motor function and metabolite concentrations in the lesioned hemispheres of arterial stroke participants. Shown are corrected concentrations (i.u.) of *N*-acetyl-aspartate (NAA) and creatine-containing compounds (Cre) in relation to four motor function tasks: (**A**) MA, Melbourne Assessment of Unilateral Upper Limb Function, (**B**) AHA, Assisting Hand Assessment, (**C**) BBT, Box and Block Test for affected and (**D**) unaffected hands. [Color figure can be viewed at wileyonlinelibrary.com]

current metabolism in these relocated sections of the motor network remains altered. This is consistent with previous evidence suggesting that since NAA turnover is complete within 2–3 days [Choi and Gruetter, 2004], MRS measurements of NAA represent current synthesis. Either interpretation (i.e., permanent vs. transient changes in NAA synthesis) may suggest further utility of perilesional NAA as a biomarker for evaluating plastic changes over time or as a result of therapeutic intervention in this population. Altered NAA concentrations could additionally or alternatively reflect changes in perilesional areas due to altered inputs from adjacent stroke regions (i.e., persisting microstructural changes in the perilesional penumbra tissue). Another possibly is diaschisis in which tissue that is spatially separated from the lesion degenerates as a result of structural connections [Kirton et al., 2016a]. The use of task fMRI to localize voxel placement aimed to obtain measurements from functional cortical motor areas. However, NAA differences may reflect alterations in cellular metabolism, tissue structure and integrity and tissue development.

TABLE III. Motor function and metabolite concentration relationships in stroke patients

	Arterial patients—Motor function measure			
Metabolite	MA	AHA	BBT-A	BBT-U
Lesioned				
NAA	$r = 0.72$, $P < 0.01$**	$r = 0.63$, $P < 0.01$**	$r = 0.71$, $P < 0.01$**	$r = 0.54$, $P < 0.05$*
Cre	$r = 0.55$, $P < 0.05$*	$r = 0.52$, $P < 0.05$*	$r = 0.65$, $P < 0.01$**	$r = 0.60$, $P < 0.05$*
Ins	$r = 0.39$, $P = 0.12$	$r = 0.47$, $P = 0.06$	$r = 0.47$, $P = 0.06$	$r = 0.64$, $P < 0.01$**
Cho	$r = 0.44$, $P = 0.08$	$r = 0.40$, $P = 0.11$	$r = 0.41$, $P = 0.10$	$r = 0.41$, $P = 0.10$
Glx	$r = 0.12$, $P = 0.65$	$r = 0.07$, $P = 0.81$	$r = 0.02$, $P = 0.95$	$r = 0.15$, $P = 0.56$
Nonlesioned				
NAA	$r = 0.50$, $P < 0.05$*	$r = 0.54$, $P < 0.05$*	$r = 0.62$, $P < 0.01$**	$r = 0.48$, $P = 0.05$*
Cre	$r = 0.33$, $P = 0.19$	$r = 0.41$, $P = 0.10$	$r = 0.51$, $P < 0.05$*	$r = 0.27$, $P = 0.28$
Ins	$r = 0.25$, $P = 0.34$	$r = 0.34$, $P = 0.18$	$r = 0.36$, $P = 0.15$	$r = 0.24$, $P = 0.36$
Cho	$r = 0.46$, $P = 0.06$	$r = 0.44$, $P = 0.08$	$r = 0.38$, $P = 0.13$	$r = 0.16$, $P = 0.54$
Glx	$r = 0.07$, $P = 0.79$	$r = 0.08$, $P = 0.75$	$r = 0.22$, $P = 0.40$	$r = 0.06$, $P = 0.81$
	PVI patients - Motor function measure			
	MA	AHA	BBT-A	BBT-U
Lesioned				
NAA	$r = 0.11$, $P = 0.73$	$r = 0.02$, $P = 0.94$	$r = -0.12$, $P = 0.72$	$r = 0.13$, $P = 0.70$
Cre	$r = 0.37$, $P = 0.24$	$r = 0.16$, $P = 0.62$	$r = -0.08$, $P = 0.81$	$r = 0.16$, $P = 0.61$
Ins	$r = 0.39$, $P = 0.21$	$r = 0.15$, $P = 0.65$	$r = 0.17$, $P = 0.60$	$r = 0.05$, $P = 0.88$
Cho	$r = 0.35$, $P = 0.26$	$r = 0.15$, $P = 0.64$	$r = -0.05$, $P = 0.89$	$r = 0.04$, $P = 0.91$
Glx	$r = -0.07$, $P = 0.83$	$r = -0.19$, $P = 0.57$	$r = -0.17$, $P = 0.61$	$r = 0.38$, $P = 0.23$
NonLesioned				
NAA	$r = 0.09$, $P = 0.79$	$r = 0.09$, $P = 0.79$	$r = 0.24$, $P = 0.45$	$r = 0.15$, $P = 0.64$
Cre	$r = 0.12$, $P = 0.71$	$r = 0.11$, $P = 0.74$	$r = 0.07$, $P = 0.83$	$r = -0.15$, $P = 0.64$
Ins	$r = 0.12$, $P = 0.70$	$r = -0.06$, $P = 0.86$	$r = 0.11$, $P = 0.74$	$r = -0.41$, $P = 0.18$
Cho	$r = 0.26$, $P = 0.41$	$r = 0.31$, $P = 0.32$	$r = 0.42$, $P = 0.17$	$r = 0.28$, $P = 0.38$
Glx	$r = 0.00$, $P = 0.99$	$r = -0.22$, $P = 0.50$	$r = -0.08$, $P = 0.80$	$r = -0.05$, $P = 0.88$

Notes: MA, Melbourne Assessment of Unilateral Upper Limb Function; AHA, Assisting Hand Assessment; BBT, Box and Block Test (BBT-A: Affected; BBT-U: Unaffected hand); NAA, *N*-acetyl-aspartate; Cre, creatine + phosphocreatine; Ins, *myo*-inositol; Cho, Glycerophosphocholine + Phosphocholine; Glx, glutamate + glutamine; *r*, Pearson partial correlation coefficient (controlling for age), * $P < 0.05$, ** $P < 0.01$.

Creatine-containing compounds were also found to be strongly associated with all measures of motor performance in children with arterial stroke. In contrast to NAA where levels in both hemispheres were associated with better motor outcome, this relationship was only seen with the lesioned motor cortex. Creatine compounds are involved in energy metabolism [Dani and Warach, 2014] and bioenergetics [Rae, 2014]. Significant concentrations of creatine are also in glial cells [Brand et al., 1993; Urenjak et al., 1993], thus increased Cre in the lesioned cortex may be due to increased Cre in cells that have a role in supporting neuronal function particularly in perilesional cortex, rather than neuronal function itself. Regardless of the cellular location of the measured Cre, higher creatine levels have been suggested to be neuroprotective and associated with enhanced cognitive functioning in some populations [Wyss and Schulze, 2002]. Given these general associations with better neurological function and the relative specificity we observed of correlations between Cre in the lesioned hemisphere (and not the contralesional tissue) and motor function, it is possible that creatine compounds reflect different elements of regional brain metabolism and health in our patient population. While requiring additional study, this represents the intriguing possibility of a functional metabolic imaging biomarker, something previously unavailable in the study of children with perinatal stroke. This result must be treated with caution as it cannot be validated with an additional reference metabolite.

Prior evidence indicates that *myo*-inositol is a glial marker [Rae, 2014] though associations with membrane phospholipid metabolism [Rango et al., 2008] and intracellular phosphoinositide second messenger systems [Rae, 2014] are also described. Elevated Ins in perilesional areas of arterial strokes where gliosis is often prominent [Yassi et al., 2016] would result in observed differences and correlations. Consistent with this hypothesis and previous studies [Cirstea et al., 2011], Ins in perilesional areas was increased in arterial stroke participants compared to the nonlesioned hemisphere

with values being symmetrical in healthy controls. Possible correlations between this biomarker and clinical motor performance were observed. This is potentially consistent with our previous observations that the relative degree of gliosis is positively correlated with motor function in children with arterial (but not venous) perinatal strokes [Kirton et al., 2013]. Taken together, this evidence suggests that glial alterations in perilesional tissue may influence motor function for which MRS measures of Ins may represent an imaging biomarker.

Choline compounds have been implicated in membrane integrity and have been suggested as a possible marker for altered cell density, neurodegeneration [Rae, 2014] or myelin breakdown [Cecil and Jones, 2001]. Our findings that choline compounds are higher in lesioned hemispheres of arterial stroke patients compared to TD is consistent with this interpretation. Perhaps also salient to our chronic stroke population is the finding that changes in normally appearing white matter in patients with multiple sclerosis show a similar elevation of choline compounds [Inglese et al., 2003]. The lack of a difference between hemispheres within patient groups may suggest there is globally increased membrane turnover and/or gliosis in these patient populations, similar to that observed in the multiple sclerosis study. These consistent findings between diseases may suggest that elevation of choline (even in normal-appearing perilesional tissue) signals underlying pathophysiology possibly indicative of altered cell density, neurodegeneration [Rae, 2014], gliosis or ischemia-induced tissue changes [Karaszewski et al., 2010].

No hemispheric differences in Glx were detected in any of our patient groups. Glx is a combined measure of glutamate and glutamine and is interpreted as a marker of glutamatergic excitation given its preponderance and its role an excitatory neurotransmitter. Glx is also known to increase with increased metabolic activity [Rae, 2014]. The lack of differences between hemispheres (lesioned vs. nonlesioned) and between groups could be due to many reasons but clinical relevance appeared less likely given that no relationship to motor function was observed. It simply indicated the success of the functional localizer and that some aspects of metabolic activation and glutamatergic exictation is "normal" in the region that is activated with motor function. Glutamate may be particularly important in motor cortex plasticity that mediates not only recovery but the ability to respond to motor learning interventions in the chronic timeframe. Combined animal and human studies have created increasingly sophisticated models of how the motor system develops following early unilateral injury [Eyre, 2007; Kirton, 2013; Staudt, 2007]. Within these, the lesioned and nonlesioned motor cortices are the primary hubs within the larger motor network with the relative balance between them being a major determinant of affected extremity function. These have recently translated into clinical trials including intensive motor learning paired with constraint therapy and noninvasive brain stimulation [Juenger et al., 2013; Kirton et al., 2016b]. Imaging biomarkers of how such interventions change the brain and which subjects may be best responders are essential to advance this field and motor cortex glutamate is an appealing candidate in need of further study.

The use of motor task-related fMRI activation patterns to place MRS voxels was performed to ensure the metabolite measurements were associated with the areas involved in performing a motor task. The correlation between GM fraction and motor function in both lesioned and nonlesioned hemispheres suggests increasing GM results in improved function, consistent with healthy populations [Jones et al., 2016]. This finding also supports that MRS voxels were successfully placed on hand regions of the primary motor cortex. A challenge in investigating neuronal plasticity, particularly in children with stroke near birth, is that motor areas traditionally anatomically defined (i.e., the hand knob of pre-central gyrus), may or may not be spatially reorganized to another location. In this sample, we found that participants with arterial strokes had more spatial variability of their voxel locations possibly reflecting developmental plasticity and reorganization in response to more extensive cortical damage compared to the PVI group. Our task fMRI driven voxel placement is a strength not often employed in such studies but issues of large lesion sizes combined with the relatively crude "real-time" fMRI method may have limited the accuracy of voxel placement. In addition, functional cortical motor areas may not always be in a single location, particularly in the nonlesioned hemisphere where reorganization patterns differ across subjects and may be complex.

Related to neuroplastic reorganization, we also found ipsilateral activations during the fMRI tapping task in some children. One interpretation of the presence of BOLD activations in the ipsilateral primary motor cortex during tapping is the recruitment of nonlesioned motor areas in the control of both hands. Clinically this sometimes manifests as "mirror movements" in which the opposite hand that the child is trying to move "mirrors" the intentional movement of the other hand. One explanation is portions of motor cortex on the intact side are controlling both hands [Kim et al., 2003]. This is consistent with our findings that performance on a seemingly unimanual task (i.e., BBT-Affected) was correlated with metabolite concentrations in ipsilateral (nonlesioned) motor areas (Table III). An in-depth exploration of ipsilateral activations and network connections is beyond the scope of the current manuscript but would be fascinating to explore in future.

An additional limitation is our smaller sample of PVI relative to arterial patients that may have reduced our ability to demonstrate differences in this group (but is reflective of naturally occurring incidence rates). We did not have clinical measures of motor function in our controls but these would not be comparable to the subjects with cerebral palsy as typically developing children ceiling (i.e., score 100%) on such measures.

The issue of selecting the most appropriate metabolite reference is challenging in MRS studies. As such, metabolite levels were reported using both water and creatine references to

address the issue of selecting an appropriate MRS reference in pediatric stroke populations within which water and creatine levels may be variable due to injury [Cecil and Jones, 2001; Rae, 2014; Schirmer and Auer, 2000] and to address chemical shift artefacts. Our study generally found consistent results between the two techniques. One exception is the NAA asymmetry between dominant and nondominant hemisphere in controls seen in water-referenced data but not Cre referenced data. This may indicate differences in the water signal or, more likely, a significant influence of chemical shift displacement artefact impacting this result. The other inconsistency between Cre and water referenced data was NAA differences between the nondominant hemisphere in controls and the contralesional hemisphere in PVI seen that was present in water-referenced but not Cre-referenced NAA. In the water-referenced data, this group difference was only mildly significant. Thus is possible that the water signal caused this difference or it may be a Type 1 statistical error, as noted above the sample size of PVI is smaller. The consistency in all other metabolites suggests that the reported results are due to changes in the metabolites and not the reference (i.e., water or Cre signal). Further supporting this interpretation is the observation that glutamate did not differ between any groups. It has been suggested that Cre is an inappropriate reference for pediatric stroke populations specifically [Cecil and Jones, 2001], the consistency of our findings between the water and Cre referenced results strengthens our findings.

Conclusions

Interrogation of motor cortex neuronal metabolism guided by fMRI activations in children with perinatal stroke-induced cerebral palsy is feasible. NAA, Ins and creatine compounds appear to be sensitive biomarkers for identifying differences between lesioned and nonlesioned hemispheres. Clinical motor function is significantly related to motor cortex metabolite concentrations of NAA and creatine compounds in children with perinatal stroke. Proton MRS may be a valuable tool in understanding the neurophysiology of developmental neuroplasticity in children with cerebral palsy.

CONFLICTS OF INTEREST

None of the authors has any conflicts of interest to declare.

REFERENCES

Albers GW, Thijs VN, Wechsler L, Kemp S, Schlaug G, Skalabrin E, Bammer R, Kakuda W, Lansberg MG, Shuaib A, Coplin W, Hamilton S, Moseley M, Marks MP (2006): Magnetic resonance imaging profiles predict clinical response to early reperfusion: The diffusion and perfusion imaging evaluation for understanding stroke evolution (DEFUSE) study. Ann Neurol 60:508–517.

Arner M, Beckung E, Eliasson A, Krumlinde-sundholm L, Rosenbaum P, Rosblad B (2005): Manual ability classification system for children with cerebral palsy. Available at: http://www.macs.nu/

Biswal B, Yetkin FZ, Haughton VM, Hyde JS (1995): Functional connectivity in the motor cortex of resting human brain using echo-planar MRI. Magn Reson Med 34:537–541.

Bourke-Taylor H (2003): Melbourne assessment of unilateral upper limb function: Construct validity and correlation with the pediatric evaluation of disability inventory. Dev Med Child Neurol 45:92–96.

Brand A, Richter-Landsberg C, Leibfritz D (1993): Multinuclear NMR studies on the energy metabolism of glial and neuronal cells. Dev Neurosci 15:289–298.

Cecil KM, Jones BV (2001): Magnetic resonance spectroscopy of the pediatric brain. Top Magn Reson Imaging TMRI 12: 435–452.

Choi I-Y, Gruetter R (2004): Dynamic or inert metabolism? Turnover of N-acetyl aspartate and glutathione from D-[1-13C]glucose in the rat brain in vivo. J Neurochem 91:778–787.

Cirstea CM, Brooks WM, Craciunas SC, Popescu EA, Choi IY, Lee P, Bani-Ahmed A, Yeh HW, Savage CR, Cohen LG, Nudo RJ (2011): Primary motor cortex in stroke: A functional MRI-guided proton MR spectroscopic study. Stroke 42:1004–1009.

Craciunas SC, Brooks WM, Nudo RJ, Popescu EA, Choi I-Y, Lee P, Yeh H-W, Savage CR, Cirstea CM (2013): Motor and premotor cortices in subcortical stroke: Proton magnetic resonance spectroscopy measures and arm motor impairment. Neurorehabil Neural Repair 27:411–420.

Dani KA, Warach S (2014): Metabolic imaging of ischemic stroke: The present and future. AJNR Am J Neuroradiol 35:S37–S43.

Eyre JA (2007): Corticospinal tract development and its plasticity after perinatal injury. Neurosci Biobehav Rev 31:1136–1149.

Fonov V, Evans AC, Botteron K, Almli CR, McKinstry RC, Collins DL, Brain Development Cooperative Group (2011): Unbiased average age-appropriate atlases for pediatric studies. NeuroImage 54:313–327.

Gillick BT, Krach LE, Feyma T, Rich TL, Moberg K, Thomas W, Cassidy JM, Menk J, Carey JR (2014): Primed low-frequency repetitive transcranial magnetic stimulation and constraint-induced movement therapy in pediatric hemiparesis: A randomized controlled trial. Dev Med Child Neurol 56:44–52.

Harris AD, Puts NAJ, Edden RAE (2015): Tissue correction for GABA-edited MRS: Considerations of voxel composition, tissue segmentation, and tissue relaxations. J Magn Reson Imaging JMRI 42:1431–1440.

Holmefur M, Krumlinde-sundholm L, Eliasson AC (2007): Interrater and intrarater reliability of the Assisting Hand Assessment. Am J Occup Ther 61:79–84.

Holshouser BA, Ashwal S, Luh GY, Shu S, Kahlon S, Auld KL, Tomasi LG, Perkin RM, Hinshaw DB (1997): Proton MR spectroscopy after acute central nervous system injury: Outcome prediction in neonates, infants, and children. Radiology 202: 487–496.

Inglese M, Li BSY, Rusinek H, Babb JS, Grossman RI, Gonen O (2003): Diffusely elevated cerebral choline and creatine in relapsing-remitting multiple sclerosis. Magn Reson Med 50: 190–195.

Jones PW, Borich MR, Vavsour I, Mackay A, Boyd LA (2016): Cortical thickness and metabolite concentration in chronic stroke and the relationship with motor function. Restor Neurol Neurosci 34:733–746.

Juenger H, Kuhnke N, Braun C, Ummenhofer F, Wilke M, Walther M, Koerte I, Delvendahl I, Jung NH, Berweck S, Staudt M, Mall V (2013): Two types of exercise-induced neuroplasticity in congenital hemiparesis: A transcranial magnetic

stimulation, functional MRI, and magnetoencephalography study. Dev Med Child Neurol 55:941–951.
Kang DW, Roh JK, Lee YS, Song IC, Yoon BW, Chang KH (2000): Neuronal metabolic changes in the cortical region after subcortical infarction: A proton MR spectroscopy study. J Neurol Neurosurg Psychiatry 69:222–227.
Karaszewski B, Thomas RGR, Chappell FM, Armitage PA, Carpenter TK, Lymer GKS, Dennis MS, Marshall I, Wardlaw JM (2010): Brain choline concentration. Early quantitative marker of ischemia and infarct expansion? Neurology 75: 850–856.
Kim Y-H, Jang SH, Chang Y, Byun WM, Son S, Ahn SH (2003): Bilateral primary sensori-motor cortex activation of post-stroke mirror movements: An fMRI study. Neuroreport 14:1329–1332.
Kirton A (2013): Modeling developmental plasticity after perinatal stroke: Defining central therapeutic targets in cerebral palsy. Pediatr Neurol 48:81–94.
Kirton A, DeVeber G (2013): Life after perinatal stroke. Stroke J Cereb Circ 44:3265–3271.
Kirton A, deVeber G, Pontigon AM, MacGregor D, Shroff M (2008): Presumed perinatal ischemic stroke: Vascular classification predicts outcomes. Ann Neurol 63:436–443.
Kirton A, Armstrong-Wells J, Chang T, deVeber G, Rivkin MJ, Hernandez M, Carpenter J, Yager JY, Lynch JK, Ferriero DM (2011): Symptomatic neonatal arterial ischemic stroke: The International Pediatric Stroke Study. Pediatrics 128:e1402–e1410.
Kirton A, Shinde S, Wei X-C (2013): Gliosis after perinatal stroke: Quantification and outcomes. Stroke 44:A75.
Kirton A, Williams E, Dowling M, Mah S, Hodge J, Carlson H, Wei X, Ichord R, PedNIHSS Investigators (2016a): Diffusion imaging of cerebral diaschisis in childhood arterial ischemic stroke. Int J Stroke. [Epub ahead of print].
Kirton A, Andersen J, Herrero M, Nettel-Aguirre A, Carsolio L, Damji O, Keess J, Mineyko A, Hodge J, Hill MD (2016b): Brain stimulation and constraint for perinatal stroke hemiparesis: The PLASTIC CHAMPS Trial. Neurology 86:1659–1667.
Kitchen L, Anderson P, Friefeld S, MacGregor D, Curtis R, Sofronas M, Domi T, deVeber G (2003): A validation study of the pediatric stroke outcome measure. Stroke 34:316.
Kobayashi M, Takayama H, Suga S, Mihara B (2001): Longitudinal changes of metabolites in frontal lobes after hemorrhagic stroke of basal ganglia: A proton magnetic resonance spectroscopy study. Stroke J Cereb Circ 32:2237–2245.
Krumlinde-sundholm L, Eliasson A-C (2003): Development of the assisting hand assessment: A Rasch-built measure intended for children with unilateral upper limb impairments. Scand J Occup Ther 10:16–26.
Krumlinde-sundholm L, Holmefur M, Kottorp A, Eliasson AC (2007): The assisting hand assessment: Current evidence of validity, reliability, and responsiveness to change. Dev Med Child Neurol 49:259–264.
Kumar P, Kathuria P, Nair P, Prasad K (2016): Prediction of upper limb motor recovery after subacute ischemic stroke using diffusion tensor imaging: A systematic review and meta-analysis. J Stroke 18:50–59.
Lynch JK (2009): Epidemiology and classification of perinatal stroke. Semin Fetal Neonatal Med 14:245–249.
Mathiowetz V, Volland G, Kashman N, Weber K (1985): Adult norms for the box and block test of manual dexterity. Am J Occup Ther 39:386–391.
Provencher SW (2001): Automatic quantitation of localized in vivo 1H spectra with LCModel. NMR Biomed 14:260–264.
Rae CD (2014): A guide to the metabolic pathways and function of metabolites observed in human brain 1H magnetic resonance spectra. Neurochem Res 39:1–36.
Raju TN, Nelson KB, Ferriero D, Lynch JK (2007): Ischemic perinatal stroke: Summary of a workshop sponsored by the National Institute of Child Health and Human Development and the National Institute of Neurological Disorders and Stroke. Pediatrics 120:609–616.
Randall M, Johnson LM, Reddihough D (1999): The Melbourne Assessment of Unilateral Upper Limb Function. Melbourne: Royal Children's Hospital.
Rango M, Cogiamanian F, Marceglia S, Barberis B, Arighi A, Biondetti P, Priori A (2008): Myoinositol content in the human brain is modified by transcranial direct current stimulation in a matter of minutes: A ^{1} H-MRS study. Magn Reson Med 60: 782–789.
Schirmer T, Auer DP (2000): On the reliability of quantitative clinical magnetic resonance spectroscopy of the human brain. NMR Biomed 13:28–36.
Shu SK, Ashwal S, Holshouser BA, Nystrom G, Hinshaw DB (1997): Prognostic value of 1H-MRS in perinatal CNS insults. Pediatr Neurol 17:309–318.
Staudt M (2007): Reorganization of the developing human brain after early lesions. Dev Med Child Neurol 49:564.
Urenjak J, Williams SR, Gadian DG, Noble M (1993): Proton nuclear magnetic resonance spectroscopy unambiguously identifies different neural cell types. J Neurosci off J Soc Neurosci 13: 981–989.
Westlake KP, Nagarajan SS (2011): Functional connectivity in relation to motor performance and recovery after stroke. Front Syst Neurosci 5:8.
Wyss M, Schulze A (2002): Health implications of creatine: Can oral creatine supplementation protect against neurological and atherosclerotic disease? Neuroscience 112:243–260.
Yassi N, Campbell BCV, Moffat BA, Steward C, Churilov L, Parsons MW, Donnan GA, Desmond PM, Davis SM, Bivard A (2016): Association between baseline peri-infarct magnetic resonance spectroscopy and regional white matter atrophy after stroke. Neuroradiology 58:3–10
Yousry TA, Schmid UD, Alkadhi H, Schmidt D, Peraud A, Buettner A, Winkler P (1997): Localization of the motor hand area to a knob on the precentral gyrus. A new landmark. Brain J Neurol 120(Pt 1):141–157.